Colloid Polym Sci (2012) 290:531–540
DOI 10.1007/s00396-011-2573-y

ORIGINAL CONTRIBUTION

Crystallization behavior of isotactic polypropylene induced by competition action of β nucleating agent and high pressure

Gang Yang · Xiaoxi Li · Jingwei Chen · Jinghui Yang · Ting Huang · Xiuru Liu · Yong Wang

Received: 14 September 2011 / Revised: 6 December 2011 / Accepted: 8 December 2011 / Published online: 27 December 2011

Abstract Addition of β-form nucleating agent (β-NA) to isotactic polypropylene (iPP) can greatly induce the variation of the crystallization of matrix. Here, we introduce high pressure to the crystallization process of β-NA nucleated iPP. It is observed that there is a competition between the effect of high pressure and the nucleation effect of β-NA on crystallization of iPP. With the increasing of high pressure, both the contents of β-iPP and α-iPP decrease while the content of γ-iPP increases. A novel crystalline morphology of γ-iPP with the fragmentations of γ-spherulites regularly organized in a local region is observed. Namely, γ-spherulites grow on the lateral of β-NA needlelike structure. The dual nucleation effects of the special needlelike structure of β-NA towards β/α-iPP and the effect of high pressure which prevents the growth of β-iPP but promotes the growth of γ-iPP are the main mechanisms for the novel crystalline morphology of γ-iPP. Specifically, the mixed polymorphic β/γ-iPP can be achieved under a certain pressure. This possibly enlarges the application of iPP material.

Keywords Polypropylene · Crystallization · Nucleating agent · High pressure

G. Yang · X. Li · J. Chen · J. Yang · T. Huang · Y. Wang (✉)
Key Laboratory of Advanced Technologies of Materials (Ministry of Education), School of Materials Science & Engineering, Southwest Jiaotong University,
Chengdu 610031, China
e-mail: yongwang1976@163.com

X. Liu
Laboratory of high pressure physics,
Southwest Jiaotong University,
Chengdu 610031, China

Introduction

Isotactic polypropylene (iPP) is one of the most important commercial polymers due to its comprehensive chemical and physical properties, and excellent processability. Furthermore, it attracts much more attention of researchers than other polymers because of its interesting microstructures. So far, it is well known that iPP exhibits at least four different crystal modifications including monoclinic α-phase (α-iPP), the trigonal β-phase (β-iPP), the orthorhombic γ-phase (γ-iPP), and smectic (intermediate state between ordered and amorphous phase), all sharing the same threefold conformation but with different spatial arrangements of iPP chains in the crystal lattice [1–7]. α-iPP is a thermodynamically stable phase with heat of fusion of 177 J/g [8] and predominates under normal processing conditions. Both β-iPP and γ-iPP are thermodynamically metastable phases with heat of fusion of 168.5 [8] and 150 J/g [5], respectively, and only can be obtained under special conditions. For β-iPP, although the shear condition and temperature gradient provoke the nucleation and growth of β-iPP, addition of an active β-phase nucleating agent (β-NA) is proved to be the most efficient way to obtain iPP articles with high content of β-iPP [9–24]. For γ-iPP, it is already known that crystallization under high pressure (>200 MPa) is the main way to achieve high content of γ-iPP [25–28] in common iPP. Under atmospheric pressure, γ-iPP also can be provoked in a low molecular weight iPP [29] or PP copolymer with the presence of comonomer unit in the main chain [6, 30, 31], and in this condition, the relative fraction of γ-iPP is relatively smaller than that in iPP obtained under high pressure.

The nucleation and growth of γ-iPP under high pressure attracts much attention in the last decades. So far, at least two crystalline morphologies of γ-iPP have been reported based

on the microscopic observations. One is the spherulitic-like aggregates which are observed in samples crystallized under high pressure [27, 32] and the other is the form of large "featherlike" structures, apparently caused by massive self-epitaxy processes [25, 33, 34]. γ-spherulites do not show the cross-hatching feature characteristic for α-spherulites grown under atmospheric pressure, but show only a moderate branching with lamellae packed in parallel stacks and spread radially. Further results show that the (010) planes of both parent and daughter α-lamellae are good ideal substrates for epitaxial growth of γ-lamellae. Thus, the growth of γ-lamellae is most frequently initiated on some "seeds" of α-lamellae since the primary nucleation of the α-lamellae is significantly easier than that of the γ-lamellae [35, 36]. Consequently, the mechanisms suggested for the growth of γ-iPP possibly includes the branching of γ-lamellae on a radially grown γ- or α-lamellae at an angle of ca. 70° or the growth of γ-lamellae at an angle of ca. 140° on previously grown γ-lamellae [5, 25].

Recent researches also prove that nucleating agent (NA) exhibits a positive role in provoking the formation of γ-iPP. Foresta et al. [6] reported that NAs of different types were found to enhance γ-iPP crystallization under atmospheric pressure, even in high molecular weight homopolymers, and the mechanism was attributed to the crystallization occurring at higher temperatures (lower supercooling). Yin [37] found that the content of γ-phase in crystallized polypropylene copolymer samples increased initially with the increasing content of NA and reached a maximum. The competition and deposition between the α- and γ-phase were proposed to explain the variation of γ-phase content.

However, the crystallization of iPP induced by joint action of high pressure and NA are less reported [38]. During the crystallization process, the presence of NA decreases the nucleation activation energy, which leads to the crystallization of iPP occurring at relatively higher temperature (lower supercooling) on the one hand. On the other hand, the high pressure provokes the nucleation and growth of γ-iPP. This indicates that NA and high pressure most likely exhibit a synergistic effect in promoting the formation of γ-iPP. Specifically, if the NA is a highly effective β-NA for iPP, possibly there is a competition between β-iPP and γ-iPP during the crystallization process. Under a certain high pressure, one possibly obtains the mixed polymorphic β/γ-iPP material. The mixed polymorphic PP material usually exhibits the excellent comprehensive mechanical properties. For example, mixed polymorphic α/β-iPP articles exhibit good balance in tensile strength, tensile modulus, and fracture resistance [39]. Therefore, in this work, a highly effective β-NA was introduced into iPP and the nonisothermal crystallization behavior of iPP under high pressure was investigated.

Experimental part

Materials

All the materials used in this study are commercially available. iPP (F401) with a melt flow rate of 2.5 g/10 min (230 °C/2.16 kg) and a density of 0.91 g/cm^3 was supplied by Lanzhou Petrochemical, Lanzhou, China. The β-NA aryl amides derivative (trade name TMB-5, powder) with a melt temperature of 197 °C was provided by Fine Chemicals Department of Shanxi Provincial Institute of Chemical Industry, China. It has been reported in the literatures that TMB-5 has chemical structure similar to *N*,*N*′-dicyclohexyl-2,6-naphthalene-dicarboxamide (commercial name NJS) [40, 41].

Sample preparation

β-NA was first melt blended with iPP to prepare the master batch, then the master batch was diluted to obtain the expected composition (iPP with 0.2 wt.% TMB-5). The melt blending of materials was conducted on a twin-screw extruder (TSE-20A, China) at a screw speed of 200 rpm and melt temperatures of 150-170-190-200-210-210-200 °C from hopper to die. After making droplets, the pellets were put into a container and were pre-melted at temperature of 200 °C. Then the sample was transferred into a set of piston–cylinder made of tungsten carbide with a resistance coil heater. The sample was heated again to 200 °C and maintained at this temperature for 10 min to erase any thermal history. Afterwards, the desired pressure (116, 193, 270, and 347 MPa) was applied and the sample was cooled down to room temperature at a cooling rate of about 5 °C/min simultaneously. This means that the crystallization of iPP was a nonisothermal process and was induced by the joint action of high pressure and β-NA. To make a comparison, the iPP sample was prepared under the complete preparation ways.

Wide-angle X-ray diffraction

The crystalline structures of iPP and iPP/TMB-5 specimens obtained at different conditions were investigated using a wide-angle X-ray diffraction (WAXD, Panalytical X'pert PRO diffractometer with Ni-filtered Cu Kα radiation at 40 kV and 40 mA) at the continuous scanning angle range from 5° to 35°. The relative fraction of β-iPP $\left(K'_\beta\right)$ was calculated according to the relation [42]:

$$K'_\beta = I^\beta_{(300)}/(I^\beta_{(300)} + I^\alpha_{(110)} + I^\alpha_{(040)} + I^\alpha_{(130)}) \quad (1)$$

where $I^\beta_{(300)}$ is the intensity of the (300) plane of β-iPP, and $I^\alpha_{(110)}, I^\alpha_{(040)}$, and $I^\alpha_{(130)}$ are the intensities of the (110), (040), and (130) planes of the α-iPP, respectively.

Furthermore, to evaluate the relative fraction of γ-iPP ($\left(K_\gamma^{'}\right)$), the following relation was used [43]:

$$K_\gamma^{'} = I_{(117)}^{\gamma}/(I_{(117)}^{\gamma} + I_{(130)}^{\alpha}) \quad (2)$$

where $I_{(117)}^{\gamma}$ denotes the intensity of the (117) plane of γ-iPP. It should be noted that the two methodologies are the relative measurements of β-iPP and γ-iPP, respectively. Specifically, Eq. 1 is valid in β/α-iPP crystalline system, and Eq. 2 to α/γ-iPP crystalline system. However, they provide at least the variation trend of β-iPP or γ-iPP fraction when the specimen is prepared in the same way and the measurement condition is completely same. Therefore, the two methodologies are widely accepted to calculate the relative fraction of β-iPP or γ-iPP. If the sample belongs to β/γ-iPP crystalline system, the above two equations are invalid to calculate the relative fraction of both β and γ-iPP. In this condition, the relative fraction of β and/or γ-iPP was calculated according to the methodology developed by Obadal which calculates all the characteristic diffraction peaks of the three α/β/γ-iPP crystal modifications [38]:

$$K_\beta = I_{(300)}^{\beta}/(I_{(300)}^{\beta} + I_{(110)}^{\alpha} + I_{(040)}^{\alpha} + I_{(130)}^{\alpha} + I_{(117)}^{\gamma}) \quad (3)$$

And then, the sheared content of α/γ-iPP in the three-phase crystalline system can be defined as:

$$K_{\alpha+\gamma} = 1 - K_\beta$$

According to the above mentioned Eq. 2, the content of α-iPP (K_α) and γ-iPP (K_γ) in the three-phase crystalline system can be calculated as:

$$K_\gamma = K_\gamma^{'}(1 - K_\beta) \quad (4)$$

$$K_\alpha = 1 - K_\beta - K_\gamma \quad (5)$$

Differential scanning calorimetry

The melting behaviors of iPP and iPP/TMB-5 were investigated using a differential scanning calorimetry (DSC, Netzsch STA 449 C Jupiter, Germany). The weight of each sample was maintained at about 8 mg. The sample was directly heated from 30 °C to 200 °C at a heating rate of 10 °C/min in the nitrogen atmosphere.

Scanning electron microscopy

The supermolecular structures of iPP and iPP/TMB-5 were investigated using a Fei Quanta 200 environmental scanning electronic microscopy (ESEM, USA) with an accelerating voltage of 20 kV. Specimen was etched for 28 h with an etchant containing 1.3 wt.% potassium permanganate ($KMnO_4$), 32.9 wt.% concentrated sulfuric acid (H_2SO_4) and 65.8 wt.% concentrated phosphoric acid (H_3PO_4), according to the methodology developed by Olley et al. [44]. All the samples were sputter-coated with gold prior to scanning electron microscopy (SEM) characterization.

Polarized optical microscopy

The nonisothermal crystallization morphologies of iPP/TMB-5 were obtained using a polarized optical microscopy (POM, Leica DMLP) equipped with a hot-stage (Linkam). First, a sample of about 5 mg was placed between two glass slides and was heated to melt completely, then the sample was pressed to obtain a slice with a thickness of about 20 μm. Afterwards, the sample was transferred to the hot-stage with the desired temperature of 200 °C and maintained at this temperature for 5 min to erase any thermal history. Then, the sample was cooled down to room temperature at a cooling rate of 20 °C/min. The nonisothermal crystallization morphologies of the samples were taken images via a digital camera.

Results and discussion

Nonisothermal crystallization of iPP/TMB-5 under atmospheric pressure

The melting behavior and crystalline structure of β-NA nucleated iPP samples were first investigated using DSC and WAXD and the results are shown in Fig. 1. To make a comparison, the results of iPP are also shown. The nonisothermal crystallization of sample was conducted out under atmospheric pressure (marked as 0.1 MPa). From Fig. 1a, one can see that, β-NA nucleated iPP exhibits triple endothermic peaks at temperatures of 154.8, 167.7, and 170.1 °C, respectively. The first endothermic peak at relatively lower temperature (154.8 °C) is ascribed to the fusion of β-lamellae, which are induced by the TMB-5 during the nonisothermal crystallization process. Because of the special lamellae structure formed during the crystallization, β-lamellae usually exhibit lower crystal density, melting temperature, and fusion enthalpy [9]. During the DSC heating process, the first endothermic peak is always present and then considered to reflect the melting range of the more or less disordered β-lamellae. The second one at 167.7 °C is attributed to the fusion of α-lamellae which form mainly during the crystallization process through self-seeding process. For the third endothermic peak at 170.1 °C, it can be explained as follows. During the heating process of DSC measurement, although the unstable β-lamellae melt firstly, the melt temperature is smaller than the melting temperature

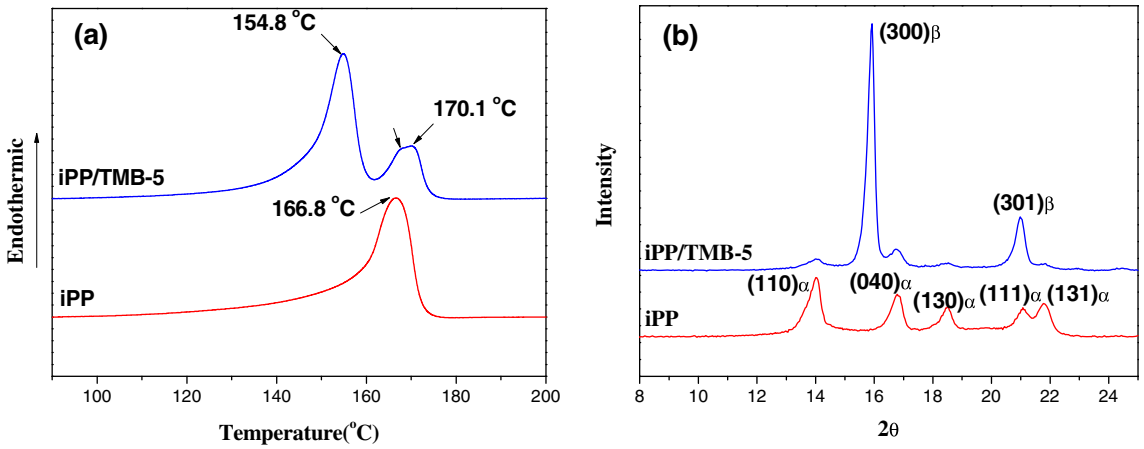

Fig. 1 **a** DSC heating curves show the melting behaviors of iPP and iPP/TMB-5, and **b** WAXD profiles show the crystalline structures of iPP and iPP/TMB-5. Samples were nonisothermal crystallized under atmospheric pressure

(T_m) of α-lamellae and some iPP chain segments still maintain the ordered structure rather than relax completely, and then these chain segments recrystallize as α-lamellae with more stable crystalline structure. Since the nucleation and growth of newly formed α-lamellae occurs at smaller supercooling degree, which is favorable for the growth of α-lamellae with bigger thickness, the newly formed α-lamellae exhibit relatively higher T_m as compared with the normal α-lamellae formed during the cooling process. In Fig. 1b, iPP/TMB-5 sample exhibits the typical characteristic diffraction peaks at 2θ=15.9° and 21.0°, indication of the (300) and (301) planes of β-iPP, respectively. The other diffraction peaks at 2θ=14.0°, 16.7°, 18.5° can be attributed to the reflection of (110), (040), and (130) planes of α-iPP, respectively. This means that although TMB-5 is an effective β-NA for iPP [19, 20, 23, 24], it does not prevent the nucleation and growth of α-lamellae. This is very important because it possibly influences the crystallization behavior of iPP/TMB-5 sample under high pressure. According to the methodology proposed by Turner-Jones [42], the K_β of iPP/TMB-5 is 0.84. By the way, from WAXD profiles, there is no trace to show the presence of γ-iPP.

Nonisothermal crystallization of PP/TMB-5 under high pressure

Figure 2 shows the WAXD profiles of different samples obtained under different pressure conditions. Similarly, the results of iPP were also shown to make a comparison. Because the 2θ values of most α-iPP diffraction peaks are similar to those of γ-iPP diffraction peaks, it is very difficult to differentiate the diffraction peaks of α-iPP and γ-iPP from WAXD profiles. Thus, the relative intensity or the areas under the two peaks, which are attributed to the diffractions of (130) plane of α-iPP at the angle of 18.5° and (117) plane of γ-iPP at the angle of 20.0°, have been taken as an indication of the content of α-iPP and/or γ-iPP. From Fig. 2a, one can see that with the introduction of high pressure during the crystallization process of iPP, one can observe a new peak at 2θ=20.0° attributing to the reflection

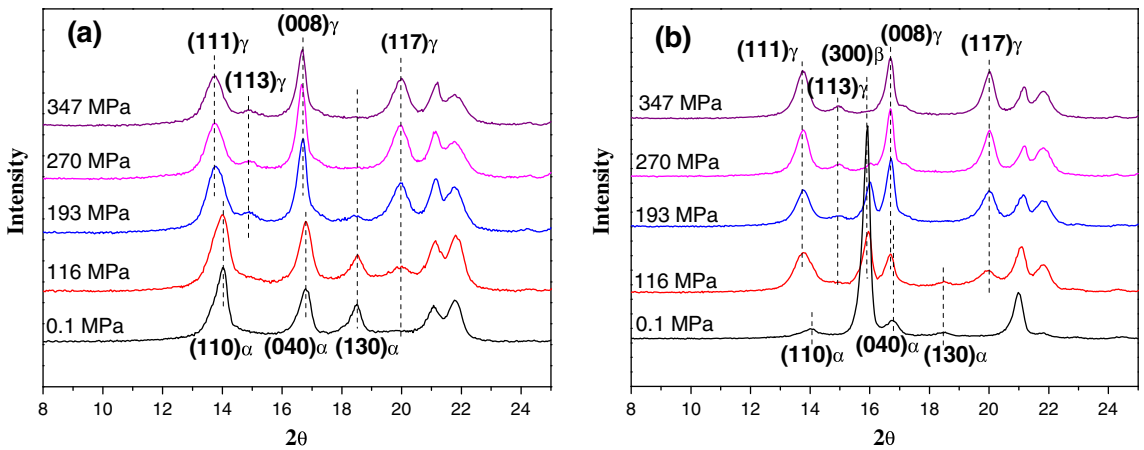

Fig. 2 WAXD profiles show the crystalline structures of **a** iPP and **b** iPP/TMB-5 samples obtained under different pressure conditions

of (117) plane of γ-iPP, indicating the presence of γ-iPP in the sample. With the increasing of applied pressure, the intensity of (117) plane becomes stronger whereas the intensity of (130) plane weakens gradually. Once the pressure is increased higher than 200 MPa, it is very difficult to differentiate the diffraction of (130) plane. However, this cannot exclude the presence of α-iPP in the sample. Considering the nucleation and growth mechanism of γ-iPP, the most possibility is that the growth of α-iPP is greatly limited to the very initial phase of crystallization process and in the formation of seeds only [32]. In this condition, the content of α-iPP is too small to be detected by WAXD measurement. By the way, under higher pressure (>193 MPa), the diffractions peaks at 2θ=13.7°, 14.9°, and 16.7° can be attributed to the reflections of (111), (113), and (008) planes of γ-iPP.

For iPP/TMB-5 sample, with the introduction of high pressure, one can still observe the diffraction peak of (117) plane. Similarly, the higher the pressure, the stronger the intensity of the diffraction peak is. Namely, the content of γ-iPP increases with the increasing of pressure. On the other hand, one can notice that the characteristic diffraction peak of (300) plane of β-iPP weakens gradually with the increasing of pressure, which indicates the decreased content of β-iPP in the sample. In other words, the nucleation effect of β-NA is weakened and the crystallization of iPP is mainly determined by pressure rather than by β-NA. Specifically, when the pressure is increased up to 347 MPa, the diffraction peak of (300) plane disappears completely and only the diffraction peaks of γ-iPP can be differentiated. Obviously, there is a competition between high pressure and β-NA in inducing the crystallization of iPP. Under atmospheric pressure and relatively lower pressure, the crystallization of iPP is mainly determined by β-NA, however, the effect of pressure on the crystallization of iPP exceeds the effect of β-NA under relatively higher pressure. The similar phenomena have been reported elsewhere [38].

Furthermore, making a comparison of crystalline structure of iPP and iPP/TMB-5 leads to more understanding about the growth of γ-iPP. For iPP sample, it still exhibits apparent diffraction peaks of α-iPP under pressure of 116 MPa as seen in Fig. 2a. However, for iPP/TMB-5 sample, the diffraction peaks of α-iPP become very weak under pressure of 116 MPa and stronger diffraction peaks of (111) and (113) planes of γ-iPP can be differentiated. Under pressure of 193 MPa, the diffraction peak of (130) plane of α-iPP in iPP sample still can be detected, while it disappears completely in iPP/TMB-5 sample. Thus, it can be deduced a route for the growth of γ-iPP in iPP/TMB-5 sample. Usually, mixed β/α-forms are observed in β-NA nucleated samples and 100% β-iPP only can be obtained using highly selective β-NA under the properly selected thermal condition of the crystallization [45]. Therefore, the chain segments which crystallize in the form of α-iPP under the atmospheric pressure are provoked to crystallize in the form of γ-iPP when the high pressure is applied during the crystallization process.

The degree of crystallinity (X_c) of the whole sample was calculated according to WAXD measurement and the results are shown in Table 1. Compared with iPP sample, the addition of β-NA enhances the X_c of iPP in iPP/TMB-5 sample slightly. However, the effect of high pressure on the X_c of iPP matrix is not significant. This further proves the route for the growth of γ-iPP in iPP/TMB-5 sample as proposed before. The relative fraction of β-iPP (K_β) cannot be calculated according to Eq. 1 when the high pressure is introduced because the diffractions peaks of (110) and (040) crystal planes cannot be differentiated. According to the methodology developed by Obadal [38], the relative fraction of both β-iPP (K_β) and γ-iPP (K_γ) was calculated and the results are shown in Table 2. It can be seen that under relatively lower pressure, the presence of β-NA promotes the nucleation and growth of γ-iPP and nucleated sample exhibits higher K_γ compared with iPP sample. However, under relatively higher pressure, the nucleated sample exhibits smaller K_γ most likely because the great nucleation effect of β-NA still promotes the formation of a few β-iPP as observed in Fig. 2b.

The melting behavior of iPP and iPP/TMB-5 obtained under different pressure conditions were characterized using DSC and the results are shown in Fig. 3. For iPP sample, the introduction of high pressure induces a shoulder on the left side of the main endothermic peak possibly due to the formation of some lamellae with smaller thickness. Under pressure of 116 MPa, the main endothermic peak locates at the temperature of 166.9 °C, which can be attributed to the fusion of α-iPP. Further increasing the applied pressure induces the decrease of the T_m. According to the WAXD measurements, the γ-iPP is the main crystalline structure when the pressure is higher than 193 MPa. Thus, the observed endothermic peak can be attributed to the fusion of γ-iPP. For iPP/TMB-5 sample, more complicated melting behavior is observed. With the increasing of applied pressure, the endothermic peak attributed to the fusion of β-iPP shifts to lower temperature and the intensity decreases gradually, indicating the decrease of the β-iPP content and the formation of some β-lamellae with smaller thickness.

Table 1 The X_c of iPP and iPP/TMB-5 obtained at different pressure conditions

Pressure (MPa)	iPP (%)	iPP/TMB-5 (%)
0.1	71.1	72.9
116	69.9	66.9
193	67.8	71.4
270	67.2	73.7
347	70.1	72.7

Table 2 The relative fraction of both β-iPP (K_β) and γ-iPP (K_γ) obtained at different pressure conditions

Pressure (MPa)	iPP (K_γ)	iPP/TMB-5 (K_γ)	iPP/TMB-5 (K_β)
0.1	0	0	0.84
116	0.51	0.58	0.38
193	0.86	0.79	0.22
270	1	0.97	0.04
347	1	1	0

Furthermore, the intensity of the endothermic peaks of two kinds of α-iPP as analyzed previously weakens gradually. This indicates at least that the content of α-iPP, whether for those formed during the nonisothermal crystallization or for those formed during the DSC heating process, decreases with the increasing of the pressure. Under pressure of 193 MPa, the endothermic peak of β-iPP becomes very weak and the endothermic peak of α-iPP is difficult to be differentiated. However, one can observe a new endothermic peak at 158.7 °C. According to the previous WAXD measurements, it can be deduced that the endothermic peak can be attributed to the fusion of γ-iPP. Further increasing pressure induces only one endothermic peak of γ-iPP. Obviously, the results of DSC agree well with those obtained from WAXD measurements.

Figure 4 shows the supermolecular structures of iPP and iPP/TMB-5 sample obtained under different pressure conditions. For iPP sample, it exhibits the typical feature of α-spherulites with a primary radial lamellae growing along the radius of the spherulites [2, 46]. With the introduction of high pressure, the typical γ-spherulites are differentiated. In these spherulites, the γ-lamellae are organized and packed in parallel stacks, spread radially and show only a moderate branching. With the increasing of pressure, the size of the γ-spherulites decreases slightly, which means that the nucleation rate of the sample is enhanced with the aid of high pressure [32]. For iPP/TMB-5 sample, it exhibits the hedritic supermolecular structure of β-iPP after being non-isothermal crystallized under atmospheric pressure. Generally speaking, the supermolecular structure of β-iPP strongly depends upon the content of β-NA, the end temperature of heating, and the thermal conditions of crystallization. Spherulitic supermolecular structure (β-spherulites) appears when crystallization takes place in a viscous state and/or at high undercooling [9]. In the presence of highly active β-NA and at high temperature isothermal crystallization process, β-iPP exhibits the hedritic supermolecular structure consisting of more or less parallel, centrally connected lamellar crystals with a polygonal appearance [47]. With the variation of the β-NA concentration, β-iPP also exhibits the different supermolecular structure: dendritic supermolecular structure at the critical content of β-NA (0.03–0.05 wt.%) and hedritic supermolecular structure at supercritical content of β-NA (>0.1 wt.%) [48–50]. In this work, the content of β-NA is 0.2 wt.%, and the sample can be thought as the "supercritically" nucleated one. A part of introduced β-NA possibly remains in the primary form, leading to the formation of a rougher and inhomogeneous supermolecular structure. Specifically, the presence of β-NA induces the crystallization occurring at relatively higher temperature, which provokes the formation of hedritic β-iPP. Under the pressure of 116 MPa, although the hedritic morphology still can be differentiated, one can notice that the size of the β-lamellae aggregates is decreased possibly because the high pressure reduces the free volume and the mobility of the chain segments and prevents the growth of β-spherulites. Furthermore, one can differentiate the presence of some γ-spherulites, although frequently immature. These γ-spherulites become more apparent under high pressure of 347 MPa. But, it should be noticed that the morphology of γ-spherulites in iPP/TMB-5 sample is rather different with that in iPP sample. This can be further proved

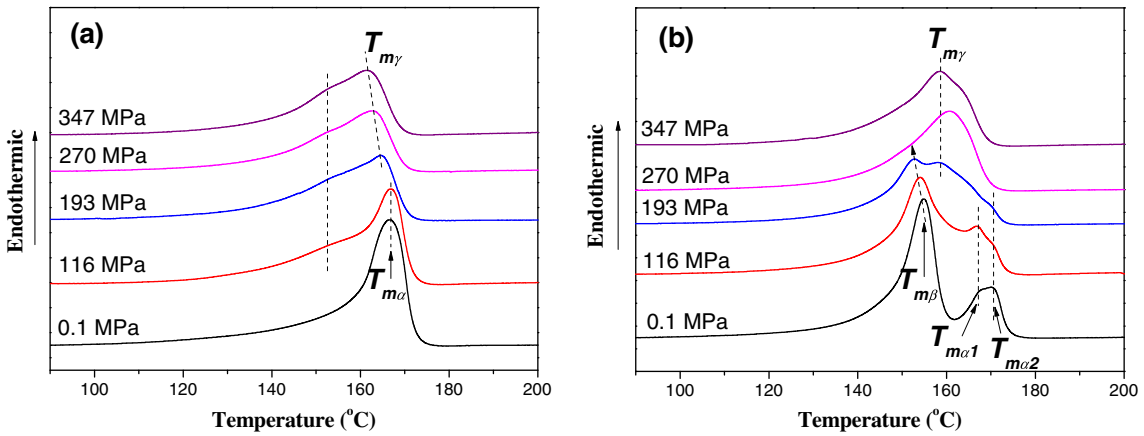

Fig. 3 DSC heating curves show the melting behaviors of **a** iPP and **b** iPP/TMB-5 samples obtained under different pressure conditions

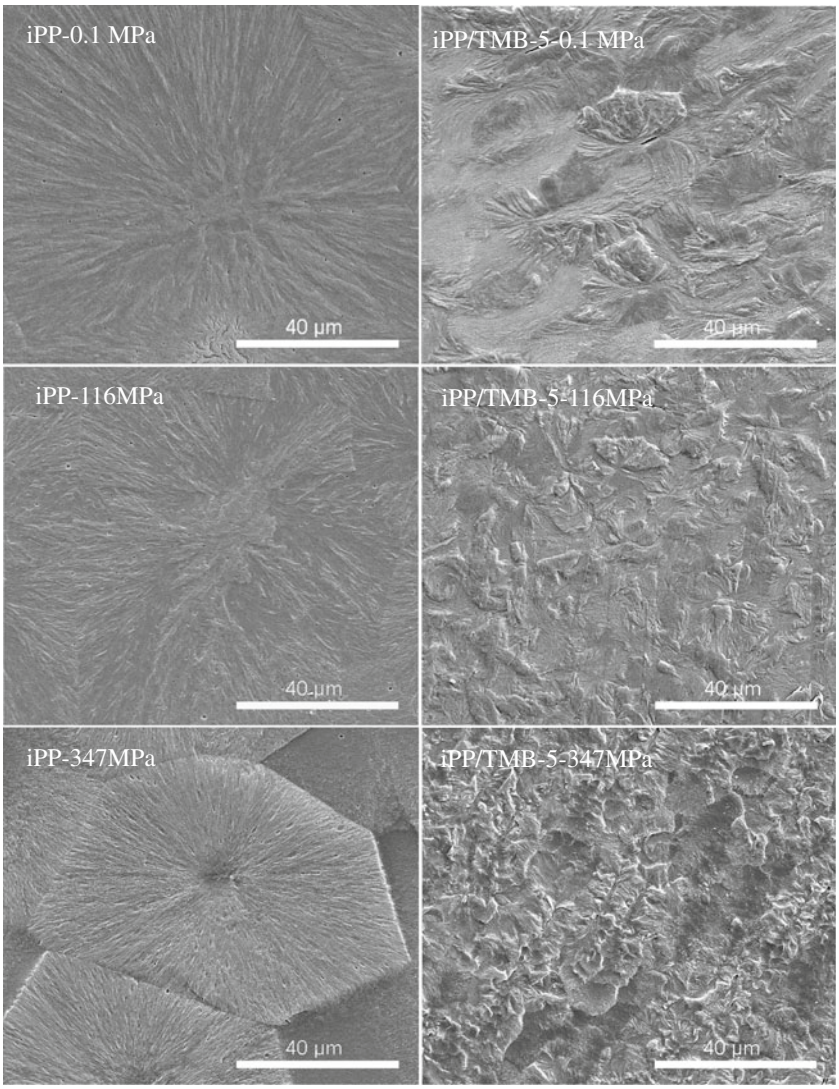

Fig. 4 SEM images show the supermolecular structures of iPP and iPP/TMB-5 samples obtained under different pressure conditions

by the supermolecular structures obtained under higher magnifications.

As shown in Fig. 5, different from the well developed γ-spherulites observed in iPP sample (Fig. 4, iPP-347 MPa),

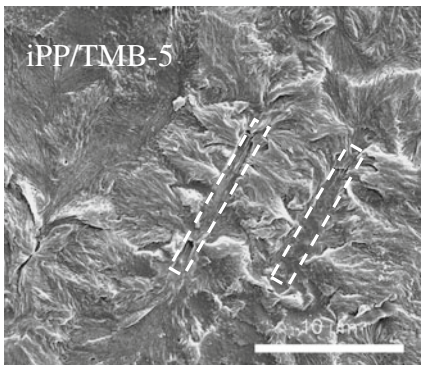

Fig. 5 SEM image at relatively higher magnification shows the supermolecular structure of iPP/TMB-5 samples obtained under high pressure of 347 MPa

the supermolecular structure of γ-iPP in iPP/TMB-5 sample exhibits at least two characteristics. The first one is that iPP/TMB-5 sample exhibits only the fragmentation of γ-spherulites, about 1/4 of the whole γ-spherulites, and the other one is that the size of γ-iPP aggregates is much smaller but the number of nucleation sites for the growth of γ-spherulites is more than that of γ-spherulites in iPP sample. Specifically, one can observe that the fragmentations of γ-spherulites are regularly organized in a local region. Namely, there is a cylinder-like crystal in the center (as shown by rectangular dash line) and some γ-spherulites grow on the lateral of it. Further results show that the cylinder-like crystal belongs to the needlelike structure of TMB-5. The similar crystal structure of TMB-5 has been reported in the literatures [41]. To the best of our knowledge, this is the first time to observe the complicated crystalline structure of γ-iPP, and the reason is believed to be the result of the joint action of high pressure and the presence of β-NA during the crystallization of iPP.

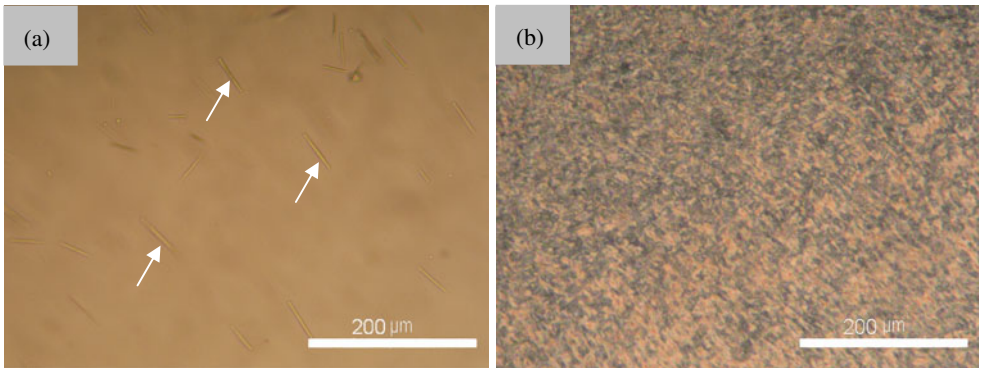

Fig. 6 **a** The needlelike structure of TMB-5 in the iPP melt at 200 °C (shown by arrows). **b** The typical nonisothermal crystallization morphology of iPP/TMB-5 sample obtained under atmospheric pressure

Further understanding about the nucleation and growth of γ-iPP in iPP/TMB-5 sample

Previously, the effect of commercial NJS on crystallization of iPP has been investigated by Varga J [48] and it was observed that a wide variety of supermolecular structure may form because of the solubility and dual nucleating ability of NJS. Specifically, an α/β-transcrystalline layer was first observed on the lateral surface of the needle crystals of NJS. As a β-NA with similar chemical structure to NJS, the morphology of TMB-5 in iPP melt depends also on the extent of solubility, associated with the content of TMB-5 and the thermal history [19, 20]. When the content of TMB-5 is higher than 0.2 wt.%, it forms the needlelike structure in the iPP melt and induces mixed polymorphic α/β-iPP transcrystalline on the lateral and β-iPP around the tip. The dual nucleation of TMB-5 for α/β-iPP has also been reported in elsewhere [51]. To further prove this, the nonisothermal crystallization morphologies of iPP/TMB-5 sample were investigated using POM and the results are shown in Fig. 6. Figure 6a shows the crystalline morphology of sample in the initial stage of the crystallization process and Fig. 6b shows the crystalline morphology of β-iPP after the completion of the crystallization. Obviously, TMB-5 forms the needlelike structure in the melt (shown by arrows). Therefore, the crystallization mechanism of iPP/TMB-5 under high pressure can be explained as follows. On the one hand, as reported in the literatures, the growth of γ-lamellae is most frequently initiated on some "seeds" of α-lamellae since the primary nucleation of the α-lamellae is significantly easier than for the γ-lamellae [35, 36, 52], especially, it has been reported that the thermodynamic driving force for the growth of γ-lamellae is very similar to that of the α-lamellae [6]; On the other hand, the addition of NA reduces the supercooling of the sample, which is favorable for the nucleation and growth of γ-lamellae. As a consequence, a schematic representation for the crystallization process is provided in Fig. 7. In the melt, TMB-5 forms the needlelike structure firstly. The annealing at 200 °C and the applied high pressure do not destroy the needlelike structure significantly. With the decreasing of the temperature, TMB-5 induces some iPP chain segments crystallize around the tip, forming the β-lamellae, and on the lateral, forming both α and β-lamellae. Under the atmospheric pressure, both the β-lamellae and α-lamellae grow simultaneously, but the former one has the larger growth

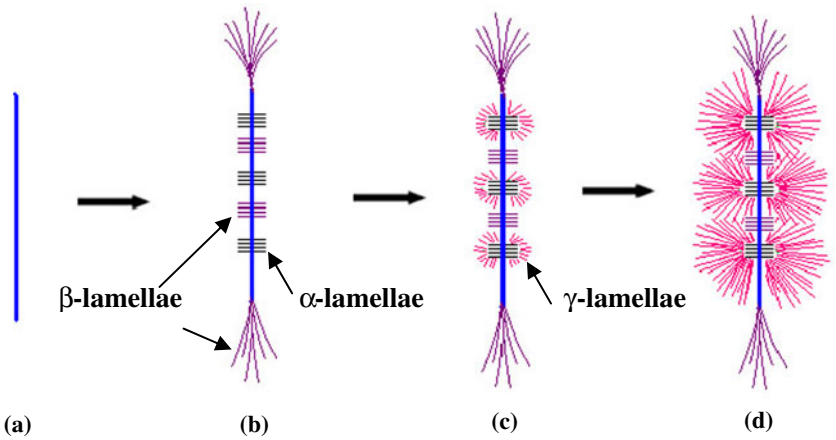

Fig. 7 Schematic representation shows the nucleation and growth of γ-iPP induced by joint action of TMB-5 and high pressure. **a** The needlelike structure of TMB-5 in iPP melt, **b** the initial stage of the nonisothermal crystallization, β-lamellae grow simultaneously around the tip and on the lateral of the needlelike structure, and α-lamellae grow on the lateral of the needlelike structure, **c** the nucleation and growth of γ-lamellae on the "seeds" of α-lamellae, and **d** the final crystallization morphology of the sample under high pressure

rate. Thus, the sample exhibits the main crystalline structure of β-iPP. However, if the crystallization occurs under high pressure, the existing α-lamellae at relatively lower supercooling act as the "seed" for the nucleation and growth of γ-lamellae, and the growth of β-lamellae is prevented, simultaneously. The higher the applied pressure, the bigger the degree of the limitation for the growth of β-lamellae is. That is the reason why only the crystalline structure of γ-lamellae under relatively higher pressure can be detected. It is suggested that there is a competition between the effect of high pressure and the nucleation effect of β-NA. DSC and WAXD do not show the presence of both β-iPP and α-iPP because the contents of them are too small to be detected. In a word, this work proves that through the joint action of β-NA and high pressure, the crystalline structure of iPP can be controlled in different degrees. Specifically, the mixed polymorphic β/γ-iPP can be achieved. This possibly enlarges the application of iPP material.

Conclusions

In summary, the nonisothermal crystallization of β-NA nucleated iPP under high pressure has been investigated. Compared to the iPP sample, the addition of β-NA induces the formation of a novel crystalline morphology of γ-iPP. With the increasing of high pressure, the contents of both β-iPP and α-iPP decrease greatly while the content of γ-iPP increases gradually. Under a certain pressure, the mixed polymorphic β/γ-iPP can be achieved. Specifically, a novel crystalline morphology with the fragmentations of γ-spherulites growing on the lateral of the cylinder-like crystal is detected. The dual nucleation effects of the special needlelike structure of β-NA towards β/α-iPP and the effect of high pressure which prevents the growth of β-iPP but promotes the growth of γ-iPP are the main mechanisms for the novel crystalline morphology of γ-iPP.

Acknowledgments The National Natural Science Foundation of China (51173151, 50973090, 11004163), Program for New Century Excellent Talents in University (NCET-08-0823), and the Fundamental Research Funds for the Central Universities (SWJTU11CX142, SWJTU11ZT10) were greatly acknowledged for financial support. Prof. Shiming Hong (Southwest Jiaotong University, China) was greatly appreciated for the help during the sample preparation process.

References

1. Binsbergen FL, De Lange BGM (1968) Morphology of polypropylene crystallized from the melt. Polymer 9:23–40
2. Lotz B, Wittmann JC, Lovinger AJ (1996) Structure and morphology of poly(propylenes): a molecular analysis. Polymer 37:4979–4992
3. Leugering HJ, Kirsch GA (1973) Effect of crystallization from oriented melts on crystal structure of isotactic polypropylene. Makromol Chem 33:17–23
4. Meille SV, Bruckner S, Porzio W (1990) γ-Isotactic polypropylene. A structure with nonparallel chain axes. Macromolecules 23:4114–4121
5. Mezghani K, Phillips PJ (1998) The γ-phase of high molecular weight isotactic polypropylene: III. The equilibrium melting point and the phase diagram. Polymer 39:3735–3744
6. Foresta T, Piccarolo S, Goldbeck-Wood G (2001) Competition between α and γ phases in isotactic polypropylene: effects of ethylene content and nucleating agents at different cooling rates. Polymer 42:1167–1176
7. O'Kane WJ, Young RJ, Bras W, Derbyshire GE, Mant GR (1994) Simultaneous SAXS/WAXS and DSC analysis of the melting and recrystallization behaviour of quenched polypropylene. Polymer 35:1352–1358
8. Li JX, Cheung WL, Jia D (1999) A study on the heat of fusion of β-polypropylene. Polymer 40:1219–1222
9. Varga J (2002) β-Modification of isotactic polypropylene: preparation, structure, processing, properties, and application. J Macromol Sci Part B Phys 41:1121–1171
10. Huo H, Jiang SC, An LJ, Feng JC (2004) Influence of shear on crystallization behavior of the β Phase in isotactic polypropylene with β-nucleating agent. Macromolecules 37:2478–2483
11. Leugering HJ (1967) Effect of crystal structure and over structure on some properties of polypropylene. Makromol Chem 109:204–216
12. Shi G, Zhang X, Qiu Z (1992) Crystallization kinetics of β-phase poly(propylene). Makromol Chem 193:583–591
13. Varga J, Mudra I, Ehrenstein GW (1999) Highly active thermally stable β-nucleating agents for isotactic polypropylene. J Appl Polym Sci 74:2357–2368
14. Ikeda N, Kobayashi T, Killough L (1996) A novel beta-nucleator for polypro-pylene. Polypropylene '96 World Congress, Zurich, Switzerland, Sept 18–20
15. Mathieu C, Thierry A, Wittmann JC, Lotz B (2002) Specificity and versatility of nucleating agents toward isotactic polypropylene crystal phases. J Polym Sci Part B: Polym Phys 40:2504–2515
16. Menyhárd A, Varga J, Molnár G (2006) Comparison of different-nucleators for isotactic polypropylene, characterisation by DSC and temperature-modulated DSC (TMDSC) measurements. J Thermal Anal Calorimetry 83:625–630
17. Krache R, Benavente R, López-Majada JM, Pereña JM, Cerrada ML, Pérez E (2007) Competition between α, β, and γ polymorphs in a β-nucleated metallocenic isotactic polypropylene. Macromolecules 40:6871–6878
18. Zhao SC, Cai Z, Xin Z (2008) A highly active novel β-nucleating agent for isotactic polypropylene. Polymer 49:2745–2754
19. Dong M, Su ZQ, Guo ZX, Yu J (2008) Study of the crystallization behaviors of isotactic polypropylene with sodium benzoate as a specific versatile nucleating agent. J Polym Sci Part B Polym Phys 46:1183–1192
20. Dong M, Guo ZX, Yu J, Su ZQ (2008) Crystallization behavior and morphological development of isotactic polypropylene with an aryl amide derivative as β-form nucleating agent. J Polym Sci Part B Polym Phys 46:1725–1173
21. Yi QF, Wen XJ, Dong JY, Han CC (2008) A novel effective way of comprising a β-nucleating agent in isotactic polypropylene (i-PP): polymerized dispersion and polymer characterization. Polymer 49:5053–5063
22. Luo F, Geng CZ, Wang K, Deng H, Chen F, Fu Q, Na B (2009) New understanding in tuning toughness of β-Polypropylene: the role of β-nucleated crystalline morphology. Macromolecules 42:9325–9331

23. Bai HW, Wang Y, Liu L, Zhang JH, Han L (2008) Nonisothermal crystallization behaviors of polypropylene with α/β nucleating agents. J Polym Sci Part B Polym Phys 46:1853–1867
24. Bai HW, Wang Y, Zhang ZJ, Han L, Li YL, Liu L, Zhou ZW, Men YF (2009) Influence of annealing on microstructure and mechanical properties of isotactic polypropylene with β-Phase nucleating agent. Macromolecules 42:6647–6655
25. Mezghani K, Phillips PJ (1997) The γ-phase of high molecular weight isotactic polypropylene. II: the morphology of the γ-form crystallized at 200 MPa. Polymer 38:5725–5733
26. Brückner S, Phillips PJ, Mezghani K (1997) On the crystallization of γ-isotactic polypropylene: a high pressure study. Macromol Rapid Commun 18:1–7
27. Angelloz C, Fulchiron R, Douillard A, Chabert B, Fillit R, Vautrin A, David L (2000) Crystallization of isotactic polypropylene under high pressure (γ phase). Macromolecules 33:4138–4145
28. Dimeska A, Phillips PJ (2006) High pressure crystallization of random propylene–ethylene copolymers: α–γ phase diagram. Polymer 47:5445–5456
29. Morrow DR, Newman BA (1968) Crystallization of low-molecular-weight polypropylene fractions. J Appl Phys 39:4944–4950
30. Pérez E, Zucchi D, Sacchi MC, Forlini F, Bello A (1999) Obtaining the γ phase in isotactic polypropylene: effect of catalyst system and crystallization conditions. Polymer 40:675–681
31. Hosier IL, Alamo RG, Esteso P, Isasi JR, Mandelkern L (2003) Formation of the α and γ polymorphs in random metallocene −propylene copolymers. effect of concentration and type of comonomer. Macromolecules 36:5623–5636
32. Lezak E, Bartczak Z, Galeski A (2006) Plastic deformation of the γ phase in isotactic polypropylene in plane-strain compression. Macromolecules 39:4811–4819
33. Yuan Q, Deshmane C, Pesacreta TC, Misra RDK (2008) Nanoparticle effects on spherulitic structure and phase formation in polypropylene crystallized at moderately elevated pressures: the influence on fracture resistance. Mater Sci Eng, A 480:181–188
34. Yuan Q, Chen J, Yang Y, Misra RDK (2010) Nanoparticle interface driven microstructural evolution and crystalline phases of polypropylene: the effect of nanoclay content on structure and physical properties. Mater Sci Eng, A 527:6002–6011
35. Lotz B, Graff S, Wittmann JCJ (1986) Crystal morphology of the γ (triclinic) phase of isotactic polypropylene and its relation to the α phase. Polym Sci Part B: Polym Phys 24:2017–2032
36. Hosier IL, Alamo RG, Lin JS (2004) Lamellar morphology of random metallocene propylene copolymers studied by atomic force microscopy. Polymer 45:3441–3455
37. Shi Q, Cai CL, Ke Z, Yin LG, Liu YL, Zhu LC, Yin JH (2008) Effect of the nucleating agent 1,3:2,4-di(3,4-dimethylbenzylidene) sorbitol on the γ phase content of propylene/ethylene copolymer. Euro Polym J 44:2385–2391
38. Obadal M, Čermák R, Stoklasa K (2005) Tailoring of three-phase crystalline systems in isotactic poly(propylene). Macromol Rapid Commun 26:1253–1257
39. Zhao SC, Xin Z (2010) Nucleation characteristics of the α/β compounded nucleating agents and their influences on crystallization behavior and mechanical properties of isotactic polypropylene. J Polym Sci Part B: Polym Phys 48:653–665
40. Dong M, Guo ZX, Yu J, Su ZQ (2009) Study of the assembled morphology of aryl amide derivative and its influence on the non-isothermal crystallizations of isotactic polypropylene. J Polymer Sci, Part B: Polymer Phys 47:314–325
41. Dong M, Guo ZX, Su ZQ, Yu J (2011) The effects of crystallization condition on the microstructure and thermal stability of isotactic polypropylene nucleated by β-form nucleating agent. J Appl Polym Sci 119:1374–1382
42. Turner Jones A, Aizlewood JM, Beckett DR (1964) Crystalline forms of isotactic polypropylene. Makromol Chem 75:134–158
43. Turner Jones A (1971) Development of the γ-crystal form in random copolymers of propylene and their analysis by DSC and X-ray methods. Polymer 12:487–508
44. Olley RH, Bassett DC (1982) An improved permanganic etchant for polyolefines. Polymer 23:1707–1710
45. Varga J (1995) Crystallization, Melting and Supermolecular Structure of Isotactic Polypropylene. In: Karger-Kocsis J (ed) "Polypropylene: Structure, Blends and Composites". Vol. I. Structure and morphology, Chapt. 3. Chapman and Hall, London, pp 56–115
46. Coulon G, Castelein G, G'Sell C (1999) Scanning force microscopic investigation of plasticity and damage mechanisms in polypropylene spherulites under simple shear. Polymer 40:95–110
47. Haeringen DT, Varga J, Ehrenstein GW, Vancso GJ (2000) Features of the hedritic morphology of β-isotactic polypropylene studied by atomic force microscopy. J Polym Sci Part B: Polym Phys 38:672–681
48. Varga J, Menyhárd A (2007) Effect of solubility and nucleating duality of *N*,*N*′-dicyclohexyl-2,6-naphthalenedicaroxamide on the supermolecular structure of isotactic polypropylene. Macromolecules 40:2422–2431
49. Kotek J, Kelnar I, Baldrian J, Raab M (2004) Tensile behaviour of isotactic polypropylene modified by specific nucleation and active fillers. Eur Polym J 40:679–684
50. Ščudla J, Raab M, Eichhorn KJ, Strachota A (2003) Formation and transformation of hierarchical structure of β-nucleated polypropylene characterized by X-ray diffraction, differential scanning calorimetry and scanning electron microscopy. Polymer 44:4655–4664
51. Na B, Lv RH, Xu W, Chen R, Zhao ZX, Yi Y (2008) Effect of nucleating duality on the formation of γ-phase in a β-nucleated isotactic polypropylene copolymer. Polym Int 57:1128–1133
52. Brückner S, Meille SU, Petraccone U, Pirozzi B (1991) Polymorphism in isotactic polypropylene. Prog Polym Sci 16:361–404